ISSN 0036-0244, Russian Journal of Physical Chemistry A, 2018, Vol. 92, No. 4, pp. 663–668. © Pleiades Publishing, Ltd., 2018.
Original Russian Text © A.N. Kalenchuk, A.E. Koklin, V.I. Bogdan, V.V. Lunin, 2018, published in Zhurnal Fizicheskoi Khimii, 2018, Vol. 92, No. 4, pp. 560–566.

CHEMICAL KINETICS AND CATALYSIS

Hydrogenation of Anthracene and Dehydrogenation of Perhydroanthracene on Pt/C Catalysts

A. N. Kalenchuk[a,b,*], A. E. Koklin[b], V. I. Bogdan[a,b], and V. V. Lunin[a]

[a] *Department of Chemistry, Moscow State University, Moscow, 119991 Russia*
[b] *Zelinsky Institute of Organic Chemistry, Russian Academy of Sciences, Moscow, 119991 Russia*
**e-mail: akalenchuk@yandex.ru*

Received March 21, 2017

Abstract—The hydrogenation of anthracene on a heterogeneous catalyst containing 3 wt % Pt/C (Aldrich) at 215, 245, and 280°C and the pressures of 40 and 90 atm is studied. The hydrogenation of anthracene to a completely hydrogenated product is considered in detail. The final product (perhydroanthracene) consists of five conformational isomers with total selectivity of more than 99%. The ratio of perhydroanthracene isomers in the end product is shown to be determined by the conditions (*P*, *T*) of hydrogenation. The rate of hydrogenation is found to slow upon an increase in the degree of benzene ring saturation. A mixture of perhydroanthracene isomers is dehydrogenated in an autoclave at 260–325°C on 3 wt % Pt/C catalyst (Aldrich) and in a flow reactor at 300–360°C on 3 wt % Pt/Sibunit catalyst. The reactivity of perhydroanthracene isomers in dehydrogenation is shown to differ.

Keywords: catalysis, hydrogenation of anthracene, dehydrogenation of perhydroanthracene
DOI: 10.1134/S0036024418040106

INTRODUCTION

Improving the quality of motor fuels and oils is the driving force behind the study of hydrogenation. This research began at the turn of the nineteenth and twentieth centuries, when P. Sabatier (France) and N.D. Zelinsky (Russia) and their colleagues discovered the catalytic hydrogenation of organic compounds at ordinary pressure and developed its fundamentals. The accelerating effect of hydrogen pressure on hydrogenation reactions was later established by Ipat'ev (Russia) [1]. Catalytic hydrogenation conducted according to Ipat'ev's concept is now an important tool in the production of safe petroleum fuels, since the content of highly carcinogenic and toxic aromatic and polyaromatic hydrocarbons (PAHs) is deliberately reduced [2]. More recently, with the development of environmental energy technologies based on fuel cells, interest in reversible hydrogenation-dehydrogenation of aromatic hydrocarbons as a source of chemically pure hydrogen has been aroused. Tremendous volumes of hydrogen are accumulated and released in these reactions. According to quantum mechanical calculations, this property of aromatic compounds becomes more pronounced as the degree of condensation increases [3].

In reactions of hydrogenation and dehydrogenation, PAHs with two condensed rings, naphthalene ($C_{10}H_8$) and decalin ($C_{10}H_{18}$), are among the ones most studied [4, 5]. Hydrogenation processes involving anthracene and the PAHs with higher degrees of condensation, resulting in an increase in the number of intermediates, are not as well studied [6–9]. The reverse dehydrogenation of saturated analogs of these PAHs remains virtually unstudied. In a review on the hydrogenation of anthracene (AN, $C_{14}H_{10}$) [7], the conversion to DHA (9,10-dihydroanthracene, $C_{14}H_{12}$) on a copper catalyst was shown to take place at 120–150°C and 120 atm. Higher temperatures and pressures are required for the subsequent formation of other reaction products:

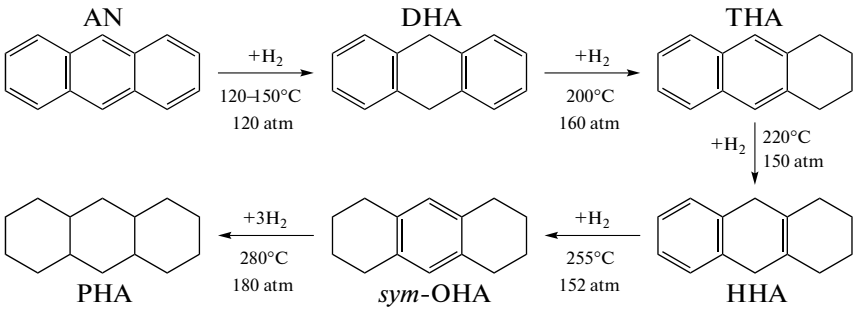

A high yield of DHA was achieved on a modified $Cu–Cr_2O_3$ catalyst under milder conditions (T = 100°C, P = 95 atm). However, conversion to THA (1,2,3,4-tetrahydroanthracene, $C_{14}H_{12}$) occurred at 240–260°C. On Ni/kieselguhr catalyst [8], all intermediates were obtained at 180–220°C and 98 atm, though a fresh portion of the catalyst was required for the end product (perhydroanthracene (PHA, $C_{14}H_{24}$)) to be formed. In [9], the formation of PHA with a selectivity greater than 25% was observed upon the hydrogenation of anthracene on a Pd/C catalyst at 300°C and 30 atm.

In a supercritical CO_2 medium (69 atm), complete conversion in anthracene hydrogenation on a Ni-containing zeolite catalyst was observed at 100°C, with a mixture of intermediates (DHA, THA and *sym*-OHA (1,2,3,4,5,6,7,8-octahydroanthracene, $C_{14}H_{18}$)) being formed [10]. The conversion of anthracene to *sym*-OHA on Pd and Rh-containing catalysts (i.e., metal nanoparticles embedded in a silicate sol–gel matrix) was described in [11]. Selectivity greater than 60% was achieved at 80°C and a hydrogen pressure of 28 atm. The conversion of anthracene to DHA on nanoparticles of Rh and Ir embedded in aluminum oxyhydroxide nanofibers under ambient conditions was reported in [12]. However, more harsh reaction conditions and an increased concentration of the active component are required for other reaction products to be obtained. Catalytically active carbon was used in [13, 14]. Molecular hydrogen was dissociated into hydrogen atoms on the catalyst's surface, followed by the transfer of hydrogen to the aromatic ring of anthracene. When using similar nonmetal catalysts, a high yield in conversion of anthracene to DHA and THA was observed at 300°C.

In addition to decalin, a great many studies have been devoted to the dehydrogenation of perhydroethylcarbazole [15], its hydrogen capacity being 5.7 wt %. In [16, 17], the dehydrogenation of perhydro-*m*-terphenyl, a compound with three relatively independent benzene rings and a hydrogen capacity of more than 7 wt %, was conducted on a Pt/C catalyst.

In this work, we studied the patterns of anthracene hydrogenation up to complete saturation with hydrogen, and the reverse dehydrogenation of the resulting perhydroanthracene on Pt/C catalysts.

EXPERIMENTAL

The hydrogenation of anthracene (97%, Aldrich; $T_{m.p}$ = 218°C, $T_{b.p}$ = 340°C) was conducted in a PARR-5500 high pressure autoclave (United States) with an internal volume of 600 mL at stirring speed of 600 rpm. The autoclave was charged with a catalyst (10 cm^3, $\rho = 0.32$ g/cm^3) and activated for 2 h in a flow of hydrogen (30 mL/min) at 305°C. Upon cooling to room temperature, the initial anthracene sample (No. 1: 100 cm^3, $\rho = 1.25$ g/cm^3) was charged into the autoclave in an inert atmosphere (N_2) and hydrogenated at 215, 245, and 280°C and pressures of 40 and 90 atm, respectively. For each discrete point, the reaction was conducted for 8 h until a completely hydrogenated product was obtained (sample No. 2). It was then analyzed. In addition, a completely hydrogenated product was obtained via the hydrogenation of another anthracene sample (No. 3: 100 cm^3, $\rho = 1.25$ g/cm^3) under steady-state conditions at 280°C and 90 atm (sample No. 4). In both cases, a Pt/C catalyst (3 wt % Pt, Aldrich) based on nanoscale carbon was used.

The completely hydrogenated product (sample No. 2) was dehydrogenated in the autoclave using a Pt/C catalyst (3 wt % Pt, Aldrich). The reaction was conducted in a continuous regime in the temperature range of 260–325°C at a pressure of 1 atm. For analysis, the resulting liquid and gaseous reaction products were released and sampled via the outlet valve.

Sample No. 4 was dehydrogenated in a high-flow catalytic converter using a Pt/C catalyst (3 wt % Pt, Sibunit) prepared by impregnating a carrier with an aqueous solution of $[H_2PtCl_6]$ ($\omega_{Pt} = 36.3\%$) [18]. The reaction was conducted in a continuous mode in the temperature range of 300–360°C at a substrate feed rate about 1 h^{-1} (linear rate, 6 mL/h; catalyst volume, 12 cm^3; catalyst bulk density, 0.67 g/cm^3). The catalyst was preliminarily activated for 2 h in a flow of hydrogen (30 mL/min) at 320°C.

The products of hydrogenation and dehydrogenation were analyzed using a KrystaLux-4000M chromatograph (Russia) equipped with a ZB-5 capillary column (Zebron, United States), a flame ionization detector, and a FOCUS DSQ II GC-MS (Thermo Fisher Scientific, United States) equipped with a TR-5MS capillary column (Thermo, United States).

Conversion (X) and selectivity (S) of the reaction products were calculated according to the formulas $X = (c_0 - c)/c_0 \times 100\%$; $S = \sum c(i)/\sum c(k) \times 100\%$, where c_0 and c are the initial and final concentrations of the initial substrate, and $\sum c(i)$ and $\sum c(k)$ are the sums of the concentrations of the individual and combined reaction products, respectively.

RESULTS AND DISCUSSION

The data show that the complete saturation of anthracene with hydrogen proceeded through several stages, the conditions for the formation of each intermediate being different. To determine the optimum conditions providing the highest end product (perhydroanthracene) yield, anthracene was hydrogenated (sample No. 1) at different temperatures and pressures.

The hydrogenation of anthracene was conducted at 215, 245, and 280°C and pressures of 40 and 90 atm. The temperature dependencies of anthracene conversion and the yield of completely hydrogenated product are shown in Fig. 1. The experimental data were com-

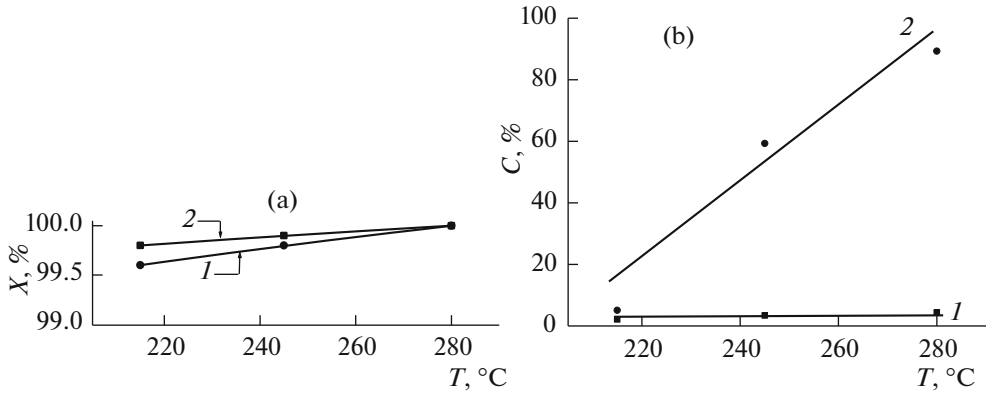

Fig. 1. Temperature dependences of (a) the conversion (X) of anthracene hydrogenation and (b) the yield (C) of perhydroanthracene at pressures of (*1*) 40 and (*2*) 90 atm.

pared and no notable effect of pressure at these temperatures on the conversion of anthracene hydrogenation (Fig. 1a) to the intermediates was found. However, the yield of the completely saturated product (Fig. 1b) grew considerably along with the pressure.

According to the results from our analysis, the following intermediates formed during the hydrogenation of anthracene: (*1*) AN; (*2*) DHA; (*3*) THA; and (*4*) three isomers of OHA, 1,2,3,4,5,6,7,8-OHA (*sym*-OHA), 1,2,3,4,4aa,9,10,10a-OHA, and 1,2,3,4,4aa,9,9aa,10-OHA (*trans* and *cis*-OHA). No hexahydroanthracene ($C_{14}H_{16}$) and decahydroanthracene ($C_{14}H_{20}$) were detected among the reaction products. The product of complete hydrogenation of anthracene (sample No. 2) was a mixture of five isomers of PHA (*5*) with a total selectivity of more than 99%. According to the order of the elution chromatographic peaks, the quantitative distribution of the isomers was PHA-*5.1*, 24.3 wt %; PHA-*5.2*, 1.4 wt %; PHA-*5.3*, 64.5 wt %; PHA-*5.4*, 4.2 wt %; and PHA-*5.5*, 6.6 wt %. Sample No. 2 was a transparent liquid

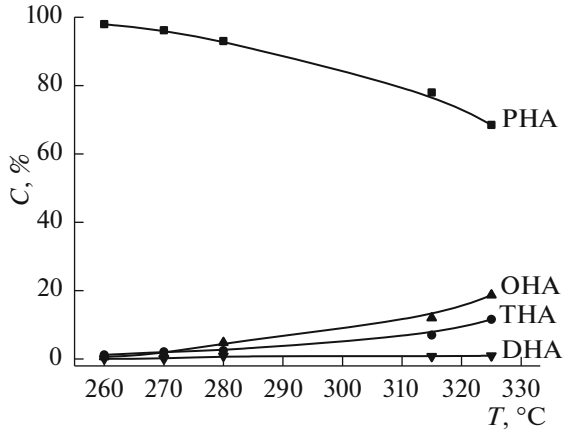

Fig. 2. Temperature dependences of the concentration (C) of perhydroanthracene and products of its dehydrogenation ($P = 1$ atm).

that did not crystallize for several months, this being in agreement with the literature data [19, 20]. Sample No. 2 was additionally subjected to elevated temperature (280°C) at a hydrogen pressure of 90 atm for 4 h. This resulted in an increase in PHA-*5.1* isomer content with a reduction in the content of all other isomers.

The pressure and temperature were brought down after sample No. 2, the product of anthracene (sample No. 1) hydrogenation, was analyzed. Dehydrogenation was then conducted in the same reaction medium in the autoclave. The data on the dehydrogenation of a mixture of PHA isomers (sample No. 2) in the range of 260–330°C are shown in Fig. 2. A close to linear decline in PHA content, accompanied by the simultaneous formation of all intermediates (OHA, THA, and DHA), was observed. No anthracene was detected among the reaction products under these conditions.

In light of our results, the repeated hydrogenation of anthracene (sample No. 3) was performed in a stationary regime at 280°C and 90 atm (Fig. 3).

The characteristic maxima on the time dependence curves of the content of reaction products show that DHA (Fig. 3, curve I-*2*), THA (Fig. 3, I-*3*), and the isomers of *sym*-OHA (Fig. 3, II-*4.1*), *trans*-OHA (Fig. 3, II-*4.2a*) and *cis*-OHA (Fig. 3, II-*4.2b*) are intermediates in the formation of the end PHA (Fig. 3, III-*5*). A comparison of the slope angles in Fig. 3 showed the relative rates of formation for each intermediate to fall as they become increasingly saturated with hydrogen.

The order of elution and time of the peaks characterizing intermediates in Fig. 3 were compared. Experimental curves (I), (II), and (III) differ distinctly in terms of the degree of saturation of aromatic rings of anthracene with hydrogen. DHA and THA are compounds with one cyclohexane ring (I), this being in agreement with our calculations. The hydrogenation of the first benzene ring was determined by the presence of two reaction sites. The plane structure of anthracene molecule was distorted due to the influence of two terminal benzene rings on the central ring,

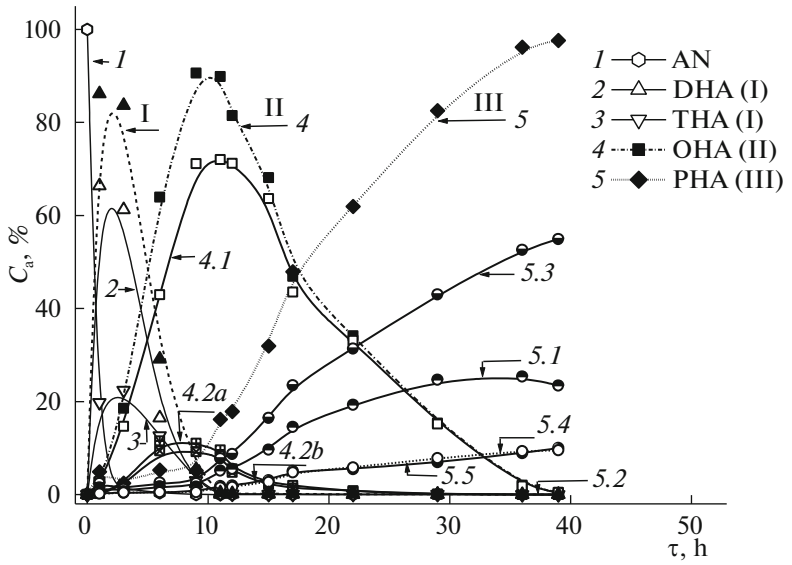

Fig. 3. Time dependences of the concentration of anthracene (C_a) and its products of hydrogenation ($T = 280$°C; $P = 90$ atm).

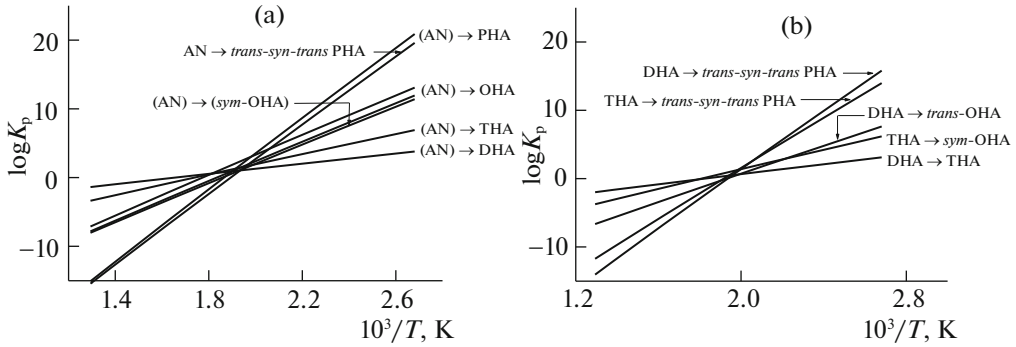

Fig. 4. Equilibrium constants (K_p) of simple kinetic-type reactions in the hydrogenation of anthracene into each intermediate.

and reaction sites emerged. As a result, the yield and relative rate of DHA formation at these sites, determined from the slope of the experimental curve, was higher than those for THA and much higher than those for all other reaction products. The conversion of anthracene to these intermediates after one hour of hydrogenation was 95% or more.

The differences between the structures of DHA and THA determined the subsequent course of hydrogenation. The presence of a cyclohexane chair disrupts the symmetry of THA molecule and makes the reactivity of its terminal benzene ring higher than that of the central ring and the terminal rings in DHA. During the reaction, the main product with two hydrogenated rings (II) is the *sym*-isomer of OHA with a central unsaturated ring. The *cis*- and *trans*-isomers of OHA with terminal unsaturated rings form in approximately equal amounts, but ones much less than those of *sym*-OHA. A simultaneous increase in the content of three isomers of OHA and a reduction in the content of DHA and THA is observed on the curves. However, the maximum content for the *cis*- and *trans*-isomers of OHA was registered after 8 h of hydrogenation. For *sym*-OHA, it was registered after 12 h.

The end product (III) of anthracene (sample No. 3) hydrogenation was a completely hydrogenated substrate (sample No. 4) with the stoichiometric composition $C_{14}H_{24}$. The obtained substrate was a liquid that was transparent at room temperature with white crystalline inclusions. Five conformation isomers of PHA were identified in this product, the quantitative distributions of which were PHA-*5.1**, 9.9 wt %; PHA-*5.2**, 0.9 wt %; PHA-*5.3**, 55.8 wt %; PHA-*5.4**, 23.8 wt %; and PHA-*5.5**, 9.6 wt %. The total selectivity of the five isomers of PHA in sample No. 2 was over 99.5%. The time required for the complete hydrogenation of anthracene was 38 h. No compounds resulting from the cracking of benzene rings of anthracene were detected.

The structure and some physicochemical characteristics of PHA isomers are given in Table 1. The ones

Table 1. Physicochemical characteristics of perhydroanthracene isomers

Isomer	Conformation	Structure		T_m, °C [18]	T_b, °C [19]	ΔH, kJ/mol [20]
A	*trans-cisoid-trans* (*trans-syn-trans;* tst)	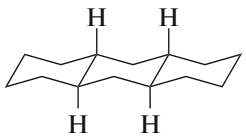	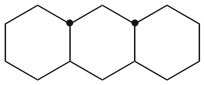	90	272–273	0
B	*trans-cisoid-cis* (*cis-transoid-trans, cis-trans*, ct)	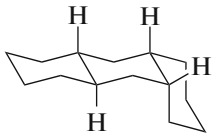	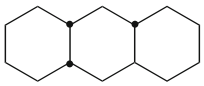	40	274–275	11.0
C	*cis-transoid-cis* (*cis-anti-cis;* cac)	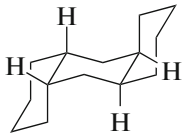	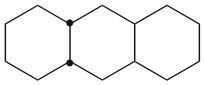	122	*	23.3
D	*cis-cisoid-cis* (*cis-syn-cis,* csc)	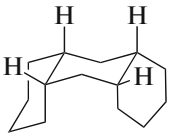	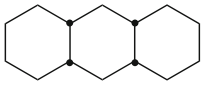	61	282–283	34.0
E	*trans-transoid-trans* (*trans-anti-trans;* tat)	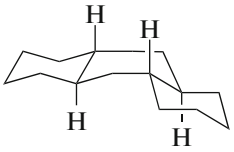	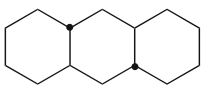	49–50	*	24.5

ΔH is enthalpy with respect to the isomer A; *no data.

most stable are the *trans-cisoid-trans* and *trans-cisoid-cis* isomers of PHA. The lower stability of the *trans-transoid-trans* isomer of PHA is due to the forced boat conformation of cyclohexane. With the *cis-cisoid-cis* isomer, it is due to sinaxial methylene interaction [21]. Isomer PHA-*5.1* was identified as *trans-cisoid-trans* (Table 1, A), and isomer PHA-*5.3* as *trans-cisoid-cis* (Table 1, B), using the mass spectra of the PHA samples (Nos. 2 and 4) and the NIST Mass Spectral Search Program for the NIST/EPA/NIH Mass Spectral Library (Version 2.0, 2005). The presence of crystalline phase in sample No. 4 would seem to be due to a high content of the *cis-transoid-cis* isomer PHA-5.4 with the highest melting point (Table 1, C). There was no detailed identification of the isomers PHA-*5.2* and PHA-*5.5*, which formed in small amounts.

Figure 4 presents the data calculated using the HSC Chemistry® 4.1 software, i.e., the theoretical equilibrium constants (K_{eq}) for the reactions of simple kinetic type that accompanied the hydrogenation of anthracene (Fig. 4a), and for the subsequent transformation of DHA and THA (Fig. 4b).

The experimental data on the formation and loss of the intermediate and end products and relative activation energies, determined from the slope in Fig. 4 for each reaction of simple kinetic type, were compared. The scheme for the hydrogenation of anthracene was then

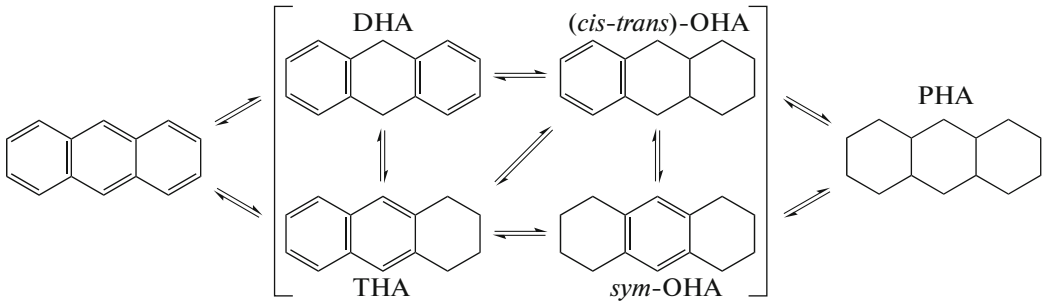

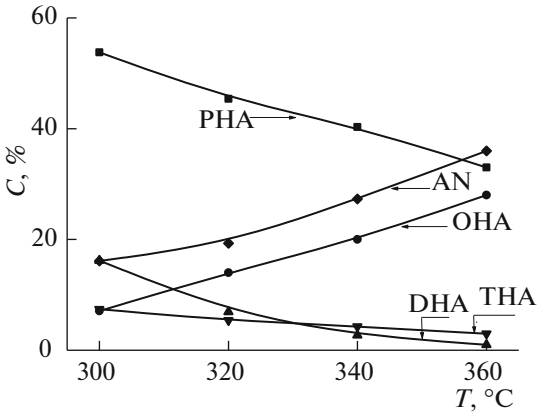

Fig. 5. Temperature dependences of the concentration (C) of dehydrogenation products for our mixture of PHA isomers in a flow reactor ($P = 1$ atm; $V_L = 1\ h^{-1}$).

It can be seen from the above scheme that the quantitative ratio of the end mixture of PHA isomers depends on the reaction pathway for anthracene hydrogenation. The pathways are in turn influenced by the reaction conditions. The compositions of the end products of anthracene hydrogenation were compared. The ratio of PHA isomers for the hydrogenation under discontinuous (sample No. 2) and stationary (sample No. 4) conditions were found to differ. Extra heating contributes to the internal isomerization of less stable isomers of PHA to a more stable *trans-cisoid-trans* conformation.

Figure 5 shows the temperature dependences of the concentrations of dehydrogenation products for the mixture of PHA isomers (sample No. 4) in the flow reactor. The total amount of all isomers of OHA and PHA is considered in these curves. From these experimental data, we can see that at 300–360°C, the main products were anthracene and the *cis*- and *trans*-isomers of OHA, with no *sym*-isomer being detected. The conversion of PHA was due to the less stable isomers PHA-*5.2*–PHA-*5.5*, while the amount of *trans-cisoid-trans* isomer (PHA-*5.1*) in this temperature range remained unchanged. A lower content of DHA and THA than that of anthracene was observed, demonstrating that the sequence in the dehydrogenation of the isomers of PHA-5.2–PHA-5.5 over cyclohexane rings (I), (II), and (III), observed when hydrogenating anthracene, was not pronounced. The complete conversion of PHA to the initial anthracene shifted to a higher temperature range.

CONCLUSIONS

In studying patterns of the reversible hydrogenation-dehydrogenation of anthracene, a completely hydrogenated substrate, i.e., a mixture of five conformational isomers of PHA, was obtained with conversion of more than 99% and a total selectivity greater than 99%. Hydrogenation proceeds through the formation of intermediates (DHA, THA, and OHA). A comparison of the experimental data showed the rate of hydrogenation to slow upon an increase in the degree of saturation of the benzene rings of anthracene. The ratio of PHA isomers in the end product was shown to be affected by the conditions (P, T) of anthracene hydrogenation. Lower temperatures promote the formation of less stable conformers of PHA. Finally, the temperature conditions of the reverse dehydrogenation reaction are determined by the end ratio of the more reactive isomers and the stable *trans-cisoid-trans* isomer of PHA. The absence of cracking products would seem to be due to the neutral carbon support.

REFERENCES

1. *Catalytic Reactions at High Temperatures and Pressures,* Ed. by V. N. Ipatiev (Akad. Nauk SSSR, Moscow, Leningrad, 1900–1933) [in Russian].
2. S. Song and X. Ma, Appl. Catal. B: Environ. **41**, 207 (2003).
3. US Patent No. 7101530.
4. C. M. Lu, Y. M. Lin, and I. Wang, Appl. Catal. A: Gen. **198**, 223 (2000).
5. Wang Bo, D. W. Goodman, and G. F. Froment, J. Catal. **253**, 228 (2008).
6. Z.-G. Zhang, K. Okada, M. Yamamoto, et al., Catal. Today **45**, 361 (1998).
7. *Handbook of Heterogeneous Catalytic Hydrogenation for Organic Synthesis,* Ed. by Sh. Nishimura (Wiley, New York, 2001), p. 477.
8. H. I. Waterman, J. J. Leenderste, and A. C. Cranendonk, Recl. Trav. Chim. Pay-Bas. **59**, 83 (1939).
9. J. L. Pinilla, A. B. Garcia, K. Philippot, et al., Fuel **116**, 729 (2014).
10. E. Sahle-Demessie, V. G. Devulapelli, and A. A. Hassan, Catalysts **2**, 85 (2012).
11. R. Abu-Reziq, D. Avnir, I. Miloslavski, et al., J. Mol. Catal. A: Chem. **185**, 179 (2002).
12. I. S. Park, M. S. Kwon, K. Y. Kang, et al., Adv. Synth. Catal. **349**, 2039 (2007).
13. F. Rodriguez-Reinoso, Carbon **36**, 159 (1998).
14. Z. G. Zhang and T. Yoshida, Energy Fuels **15**, 708 (2001).
15. Z. H. Wang, I. Tonks, J. Bell, et al., J. Organomet. Chem. **694**, 2854 (2009).
16. V. I. Bogdan, A. N. Kalenchuk, and L. M. Kustov, in *Proceedings of the 12th European Congress on Catalysis–EuropaCat-XXII, Kazan, Russia, 2015,* p. 1088.
17. A. N. Kalenchuk, V. I. Bogdan, and L. M. Kustov, Catal. Ind. **7**, 60 (2015).
18. R. L. Clarke, J. Am. Chem. Soc. **83**, 965 (1961).
19. J. W. Cook, N. A. McGinnis, and S. Mitchell, J. Chem. Soc., 286 (1944).
20. N. L. Allinger and M. T. Wuesthoff, J. Org. Chem. **36**, 2051 (1971).
21. *Basic Organic Sterochemistry,* Ed. by E. I. Iliel, S. H. Wilen, and M. P. Doyle (Wiley International, New York, 2007), p. 507.

Translated by D. Yakusheva